THE JOURNAL OF PHYSICAL CHEMISTRY LETTERS
A JOURNAL OF THE AMERICAN CHEMICAL SOCIETY

Open Access
This article is licensed under CC-BY 4.0

pubs.acs.org/JPCL
Letter

Experimental Characterization of the Isomer-Selective Generation of the Astrochemically Relevant Hydroxymethylene Radical Cation ($HCOH^{\bullet+}$/$DCOH^{\bullet+}$)

Vincent Richardson,* Luke Alcock, Nicolas Solem, David Sundelin, Claire Romanzin, Roland Thissen, Wolf D. Geppert, Christian Alcaraz, Miroslav Polášek, Brianna R. Heazlewood, Quentin Autret, and Daniela Ascenzi

Cite This: J. Phys. Chem. Lett. 2024, 15, 10888−10895

Read Online

ACCESS | Metrics & More | Article Recommendations | Supporting Information

ABSTRACT: Interest in the observation and characterization of organic isomers in astronomical environments has grown rapidly with an increase in the sensitivity of detection techniques. Accurate modeling and interpretation of these environments require experimental isomer-specific reactivity and spectroscopic measurements. Given the abundance of formaldehyde (H_2CO) in various astrophysical objects, the properties and reactivities of its cation isomers $H_2CO^{\bullet+}$ and $HCOH^{\bullet+}$ are of significant interest. However, for the hydroxymethylene radical cation $HCOH^{\bullet+}$ (and its isotopologue $DCOH^{\bullet+}$), detailed reactivity studies have been limited by the lack of suitable experimental methods to generate this isomer with high purity. Here, potential approaches to the isomer-selective generation of $HCOH^{\bullet+}$ and $DCOH^{\bullet+}$ are characterized through differential reactivity measurements. While the dissociative photoionization of cyclopropanol (c-CH_2CH_2CHOH) is determined to be unsuitable, the dissociation of methanol-d_3 (CD_3OH) allows for the formation of $DCOH^{\bullet+}$ with a fractional abundance of >99% at photon energies below 14.8 eV. These results will allow future spectroscopic and reactivity measurements of $HCOH^{\bullet+}$/$DCOH^{\bullet+}$ to be conducted, laying the groundwork for future detection and incorporation into models of the interstellar medium.

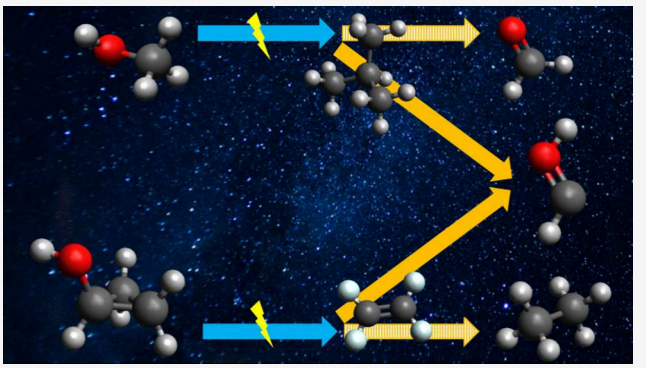

Following the determination of the relative abundances of the HCO^+/HOC^+ and $HCN^{\bullet+}$/$HNC^{\bullet+}$ isomeric ion pairs in the interstellar medium (ISM),[1−4] there has been a growing acknowledgment of the importance of isomerism and experimental isomer-specific reactivity measurements in astrochemistry.[5,6] Isomerization barriers that are sufficiently small to allow for isomers to exist in equilibrium under terrestrial conditions can be prohibitive at the lower temperatures present in many astrochemical environments, such as dark clouds. Conversely, for some species, the higher energy isomer is found to be the most abundant, a situation that is unlikely under terrestrial conditions. As such, the differing chemical and spectroscopic properties of isomers necessitate isomer-specific laboratory measurements in order to accurately model and interpret the chemistry of astronomical environments.

Isomer-selective reactivity has been shown to be of particular importance to the modeling of planetary and satellite atmospheres, with a notable example being the contribution of different $[C_3H_3]^+$ isomers to the chemistry of Titan, the largest moon of Saturn.[7] Furthermore, isomer-selective generation is also important for fundamental gas-phase kinetics measurements,[8−11] as the differing reactivities of isomers can provide important insights into the interrelationship between structure and reactivity.[12,13] This is especially significant for small radical cations where subtle changes in structure can lead to significantly different reactivity.[14−19]

Neutral formaldehyde (H_2CO) has long been known to be present in the ISM,[20] where it is routinely detected in large and varied range of astrophysical objects, from diffuse clouds[21] to protoplanetary disks[22] and protoplanetary nebulae[23] (see Appendix A in ref 24 for a list of objects where formaldehyde and its isotopologues have been detected). With an ionization energy (IE) of 10.9 eV,[25,26] it is anticipated that H_2CO will be readily ionized by UV photons, cosmic rays, and high-energy electrons. As the anticipated product ions, $H_2CO^{\bullet+}$ and

Received: August 12, 2024
Revised: September 30, 2024
Accepted: October 1, 2024
Published: October 24, 2024

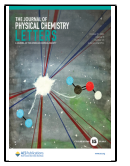

ACS Publications
© 2024 The Authors. Published by American Chemical Society

https://doi.org/10.1021/acs.jpclett.4c02374
J. Phys. Chem. Lett. 2024, 15, 10888−10895

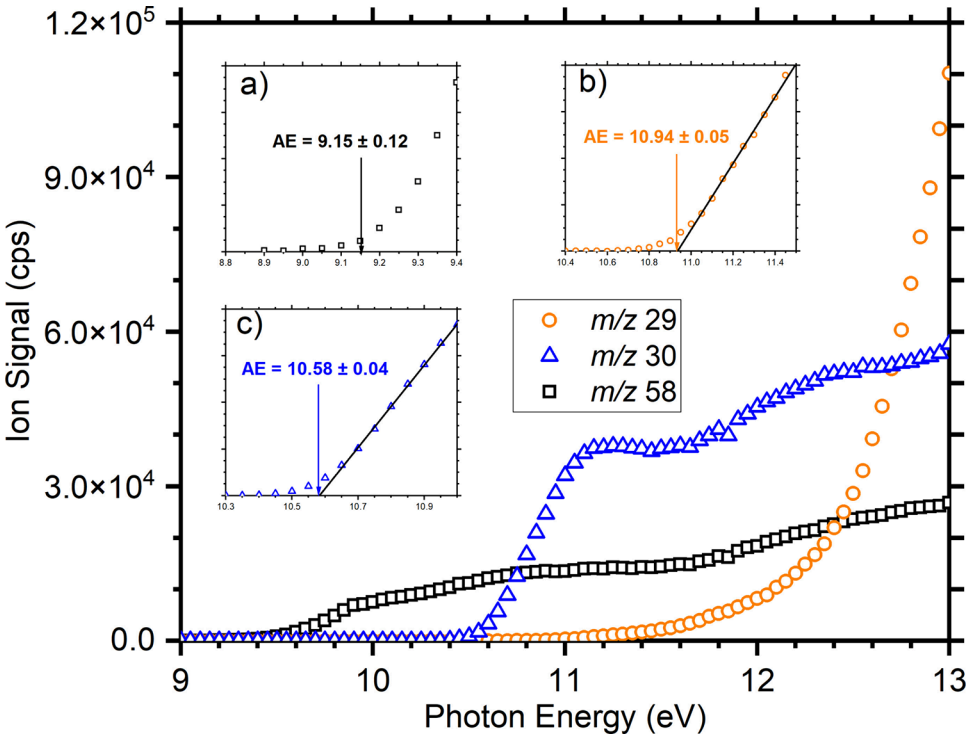

Figure 1. Photoionization efficiency (PIE) curves for the dissociative photoionization of cyclopropanol giving $[C_3H_6O]^+$ (m/z 58, black squares), $[CHO]^+/C_2H_5^+$ (m/z 29, orange circles), and $[CH_2O]^{\bullet+}/C_2H_6^{\bullet+}$ (m/z 30, blue triangles). Insets a), b), and c) show the threshold regions for the corresponding m/z values, along with the assigned appearance energies (AEs).

$HCOH^{\bullet+}$, are yet to be explicitly detected in the ISM, likely due to the highly transient nature of radical cations even in such low density environments, the need for precise laboratory-based studies of these species is clear. While the formaldehyde radical cation ($H_2CO^{\bullet+}$) is the most stable $[CH_2O]^{\bullet+}$ isomer, the *trans* and *cis* $HCOH^{\bullet+}$ isomers are only 0.3 and 0.44 eV higher in energy, respectively.[27] A third isomer, $COH_2^{\bullet+}$, will probably play a minor role in cold environments since it is more than 2 eV higher in energy than the $H_2CO^{\bullet+}$ and $HCOH^{\bullet+}$ isomers,[28] and so it is not considered further here.

Importantly, the barrier to isomerization between $H_2CO^{\bullet+}$ and *trans* $HCOH^{\bullet+}$ of 1.97 eV is higher in energy than that for the fragmentation into HCO^+ plus H, meaning that interconversion over this barrier is highly unlikely. Furthermore, a recent computational study[29] determined the tunneling lifetime of the $HCOH^{\bullet+}$ isomer to be on the order of thousands of years at representative ISM temperatures. Given this, formation mechanisms such as the protonation of HCO,[30] radical hydrogen abstraction from H_2COH^+,[31] or dissociative charge transfer reactions with methanol[32,33] have the potential to form a mix of the two $[CH_2O]^{\bullet+}$ isomers under the low temperature conditions typical of the ISM.

While the production of $H_2CO^{\bullet+}$ (e.g., by ionization of H_2CO) has been amply investigated,[34,35] the generation of $HCOH^{+\bullet}$ (and its isotopologue $DCOH^{+\bullet}$) is less straightforward and has been the subject of significant research interest due to its implications for both astrochemistry and fundamental reaction dynamics. Furthermore, it is notable that the characterization of the isomer-selective generation of neutral HCOH has been reported only very recently.[36] While the dissociative ionizations of cyclopropanol (c-CH_2CH_2CH-(OH)),[37,38] methanol (CH_3OH),[38−40] and trideuterated methanol (CD_3OH)[17,38] have been suggested as suitable methods for generating the $HCOH^{+\bullet}$ isomer, or its partially deuterated isotopologue $DCOH^{\bullet+}$, no quantitative experimental characterization of the isomeric purity has yet been performed. Here, we present experimental results on the characterization of the isomeric purity of $HCOH^{+\bullet}$ and $DCOH^{+\bullet}$ formed from both cyclopropanol and CD_3OH for use in future ion-molecule reactivity studies.

Measurements have been performed using a guided ion beam tandem mass spectrometer, allowing for ions formed in the source chamber to be mass-selected prior to introduction into the reaction cell. By monitoring the pressure in the cell and the intensity of different parent and product mass channels, absolute cross sections (CSs) and branching ratios (BRs) can be obtained for the reactions of different parent ions. Measurements are recorded as a function of both the energy of the photons used in the dissociative photoionization process and the collision energy available to the reactants. Tunable VUV sources, in this case the DESIRS beamline[41] of the SOLEIL synchrotron radiation facility, allow for a high level of control over the photon energy. This, in turn, allows for the tuning of the internal energy of the ions formed and, by extension, the fragmentation dynamics. Full experimental details, including a discussion of the uncertainties associated with the measurements reported here, are given in the Supporting Information.

For a source generating a mixture of two different species A and B (either isomers or entirely different chemical species), the observed reaction CS of the mixture, σ_T, can be described by the following equation

$$\sigma_T = (n_A \times \sigma_A) + (n_B \times \sigma_B) \quad (1)$$

https://doi.org/10.1021/acs.jpclett.4c02374
J. Phys. Chem. Lett. 2024, 15, 10888−10895

where n_A and n_B are the fractions of A and B, respectively, while σ_A and σ_B are the absolute reaction CSs of pure samples of A and B, respectively. If σ_A and σ_B are known, then n_A and n_B can be determined for a given σ_T. Here, we have employed this approach to determine the isomeric purity, i.e., the relative yields of the $HCOH^{\bullet+}$ and $H_2CO^{\bullet+}$ isomers from different generation methods. However, due to the lack of isomer-selective reactivity data for $HCOH^{\bullet+}$ and $DCOH^{\bullet+}$, this quantification must be performed through the subtraction of the $H_2CO^{\bullet+}$ fractional abundance, for which isomer-selective generation is well-established.

The ionization of cyclopropanol has previously been shown to produce an intense m/z 30 fragment at 1−2.5 eV above the ionization threshold of 9.10 eV.[37,42] Though the m/z 30 fragment was initially assigned exclusively to the formation of $HCOH^{\bullet+}$ in combination with C_2H_4,[37] a more recent study[42] provided an alternative assigment—attributing it instead to the formation of $C_2H_6^{\bullet+}$ in combination with CO, though we note that the $HCOH^{\bullet+}$ isomer is not discussed in this study. The reattribution to $C_2H_6^{\bullet+}$ plus CO was based on the threshold energy (1.47 eV above the 9.10 eV ionization energy of cyclopropanol) being in agreement with the calculated dissociation limit of 10.57 eV, while fragmentation into $H_2CO^{\bullet+}$ plus C_2H_4 has a higher dissociation limit of 11.35 eV. A further study[38] noted that, while the m/z 30 fragment is a doublet of $C_2H_6^{\bullet+}$ and $[CH_2O]^{\bullet+}$, the $[CH_2O]^{\bullet+}$ component is consistent with the $HCOH^{\bullet+}$ isomer.

In order to benchmark our results against this previous study,[42] the appearance energies (AEs) of the relevant fragments have been measured from their respective photoionization efficiency (PIE) curves, with the results for both the parent ion (m/z 58) and the m/z 29 and 30 fragments shown in Figure 1. For the m/z 29 and 30 fragments this has been performed via linear threshold extrapolation of the PIE curve,[43−46] while, due to the lack of a well-defined onset, the AE for the m/z 58 parent ion has been determined as the first point above noise. We note that the AE values given here, and elsewhere in this work, are used only for comparison with AEs determined previously in the literature and not to derive relevant thermochemical values. For a complete discussion on the fitting of AE thresholds, please refer to Roithová et al.,[43] Ruscic,[47] and the references therein. For the m/z 58 ion, the measured AE of 9.15 ± 0.12 eV is in good agreement with the previously measured IE of 9.10 eV.[42] Similarly, the AE of the m/z 30 fragment of 10.58 ± 0.04 eV is in excellent agreement with the previous measurement of 10.57 eV.[42] Finally, the AE for the m/z 29 channel, which has previously been assigned to a mix of $C_2H_5^+$ and HCO^+, is measured as 10.94 ± 0.05 eV, in reasonable agreement with the previously reported AEs of 10.75 and 10.88 eV for the two channels, respectively.[42] Notably, the m/z 29 channel shows a sharp rise in intensity above ∼12 eV, in agreement with the observation of the previous study,[42] where it was assigned in part to the opening of the channel leading to the formation of $C_2H_5^+$ in combination with CO and $H^\bullet$, which has an AE of 11.49 eV.[42]

In order to reduce any internal energy effects while maintaining a sufficient ion yield at m/z 30, the reactivity experiments discussed below are performed at a photon energy of 11.2 eV. C_2D_4 is chosen as the neutral reactant to disentangle the presence of $C_2H_6^{\bullet+}$ from that of $[CH_2O]^{\bullet+}$. The reaction of $C_2H_6^{\bullet+}$ with C_2H_4 has been studied previously,[48] and the sole m/z 28 product ($C_2H_4^{\bullet+}$), corresponding to the charge transfer, is observed with a rate of (1.15 ± 0.12) × 10^{-9} $cm^3 \cdot molecule^{-1} \cdot s^{-1}$. C_2D_4 is chosen in preference to its undeuterated equivalent (C_2H_4) to simplify the analysis by partially deuterating product species that would otherwise be equivalent as, while the charge transfer reaction is also energetically accessible for the $H_2CO^{\bullet+}$ ion, a previous study of the reaction of this ion with C_2D_4 observed not only the charge transfer product (m/z 32, $C_2D_4^{\bullet+}$), but also a distinctive combination of proton (m/z 33, $C_2D_4H^{\bullet+}$) and hydrogen atom transfer (m/z 29, HCO^+) channels.[16] As the BRs, and their relative collision energy dependencies, have been reported in detail previously,[16] consideration of the reaction of the m/z 30 fragment with C_2D_4 therefore allows for discrimination between the relative contributions of the $C_2H_6^{\bullet+}$, $H_2CO^{\bullet+}$, and $HCOH^{\bullet+}$ ions. Details of the data treatment are provided in the Supporting Information, with the resulting absolute CSs as a function of the collision energy given in Figure 2.

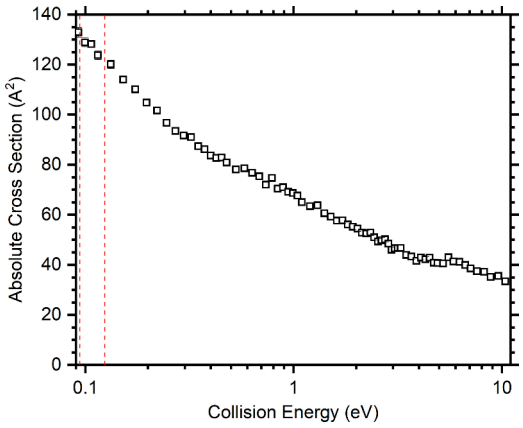

Figure 2. Summed absolute cross sections (CSs) as a function of the collision energy for the m/z 32 charge transfer product $C_2D_4^{\bullet+}$ and the corresponding secondary products at m/z 46, 62, 74, and 78, following the reaction of the m/z 30 fragment from the dissociative photoionization of cyclopropanol with C_2D_4 at E_{phot} = 11.2 eV. The red dashed lines represent the collision energy uncertainty range for the cross section used for the rate calculations, as detailed in the text.

Given CSs at a fixed collision energy, energy-dependent total rate constants can be obtained from the following expression

$$k_{tot}(E_{ave}) = \langle v \rangle \cdot \sigma_{tot} \quad (2)$$

where σ_{tot} is the absolute reaction CS and $\langle v \rangle$ is the average relative velocity obtained from the collision energy.[49,50] In order to compare the results of our measurements with those of the $C_2H_6^{\bullet+}$ ion recorded using an ion cyclotron resonance (ICR) mass spectrometer,[48] $k_{tot}(E_{ave})$ is calculated from the experimental data at a collision energy of 0.11 ± 0.02 eV, with the obtained $k_{tot}(E_{ave})$ value of (1.48 ± 0.55) × 10^{-9} $cm^3 \cdot molecule^{-1} \cdot s^{-1}$ being in good agreement with the literature value of (1.15 ± 0.12) × 10^{-9} $cm^3 \cdot molecule^{-1} \cdot s^{-1}$ for the reaction of the $C_2H_6^{\bullet+}$ ion.

While we do observe minor products at m/z 33, 60, and 61 that are indicative of the presence of $[CH_2O]^{\bullet+}$, we conclude that the majority of the m/z 30 fragment ion signal does indeed correspond to the formation of $C_2H_6^{\bullet+}$. This conclusion is reached through comparison of the observed m/z 32 (and subsequent secondary reaction) CSs with those of previous studies on the reaction of $C_2H_6^{\bullet+}$. In this way, we are able to determine that the lower limit, within error, for the

https://doi.org/10.1021/acs.jpclett.4c02374
J. Phys. Chem. Lett. 2024, 15, 10888−10895

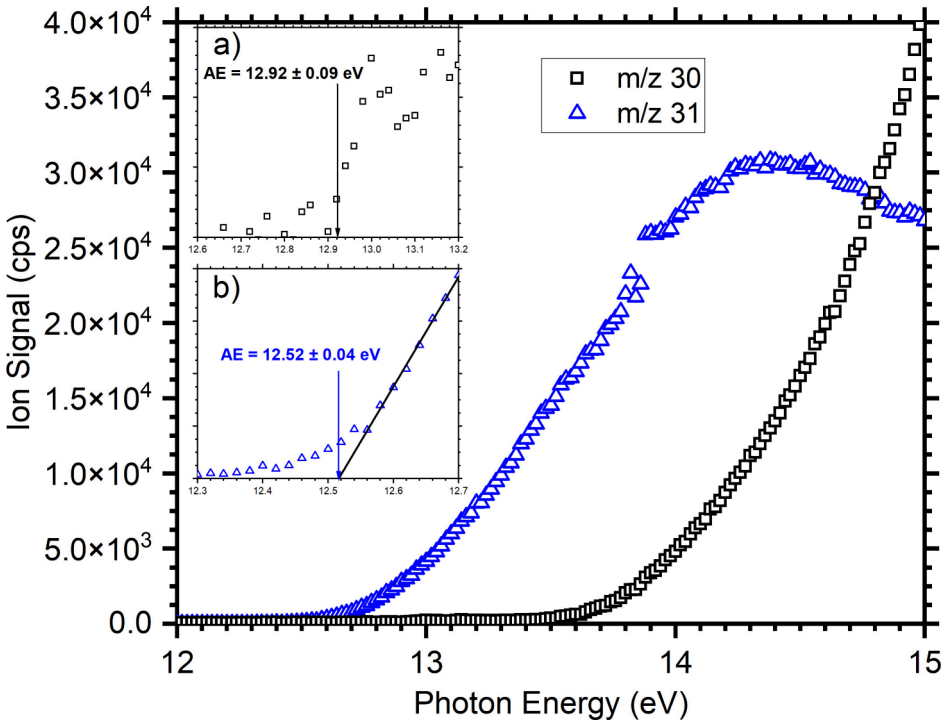

Figure 3. Photoionization efficiency (PIE) curves for the dissociative photoionization of CD_3OH giving DCO^+/COD^+ (m/z 30, black data) and $DCOH^{\bullet+}/DHCO^{\bullet+}$ (m/z 31, blue data). Insets a) and b) show the threshold regions for the corresponding m/z 30 and 31 fragments, along with the assigned appearence energies (AEs).

fraction of $C_2H_6^{\bullet+}$ present is 0.57, with an upper limit for the fraction of $HCOH^{\bullet+}$ of 0.10. The dissociative ionization of cyclopropyl alcohol is therefore disregarded as a suitable method for the selective generation of the $HCOH^{\bullet+}$ ion.

The dissociative photoionization of trideuterated methanol (CD_3OH) was first suggested by Berkowitz[40] as being preferable to the dissociative ionization of fully hydrogenated methanol due to the ability to separate the $D_2CO^{\bullet+}$ (m/z 32) and $DCOH^{\bullet+}$ (m/z 31) fragments by their mass-to-charge ratios.[17,38] However, as there is the potential for H/D exchange prior to ejection, as evidenced by the experimental observation of the D_2COD^+ fragment (m/z 34) with an AE of 11.85 eV that is below that of 12.60 eV for the m/z 31 fragment,[51] the potential for isobaric contamination from $DHCO^{\bullet+}$ has to be considered.

As with cyclopropanol, PIE curves for the m/z 30 ($[CDO]^+/[^{13}CHO]^+$) and 31 ($[CDHO]^{\bullet+}/[^{13}CDO]^+$) fragments have been measured and are presented in Figure 3. The AE of the m/z 31 channel has been determined, again using linear threshold extrapolation, to be 12.52 ± 0.04 eV, in reasonable agreement with the value of 12.6 eV recorded previously.[51] Due to a small contamination from H_2CO in the source chamber from previous measurements, the m/z 30 fragment channel has a baseline of ~100 cps, with the appearance energy of the DCO^+ channel determined from the first point above noise as 12.90 ± 0.09 eV.

For the characterization of any $DHCO^{\bullet+}$ impurity in the m/z 31 channel from deuterated methanol, isobutane ($CH(CH_3)_3$) has been selected as the reactant neutral because its IE of 10.68 ± 0.11 eV[26] is between the IEs of DHCO (the IEs of H_2CO and D_2CO being 10.889 ± 0.003 eV[25,26] and 10.908 ± 0.003 eV,[25] respectively) and HCOH, which has an IE of 8.91 ± 0.02 eV.[28] This means that the charge transfer process from $DHCO^{\bullet+}$ will be exothermic, while the charge transfer from $DCOH^{\bullet+}$ will be endothermic (and therefore closed at low collision energies in the absence of internal excitation). For this process, eq 1 can be rewritten as follows

$$\sigma_T = (n_{DHCO^{\bullet+}} \times \sigma_{DHCO^{\bullet+}}) + (n_{DCOH^{\bullet+}} \times \sigma_{DCOH^{\bullet+}}) \quad (3)$$

where $n_{DHCO^{\bullet+}}$ and $n_{DCOH^{\bullet+}}$ are the isomeric fractions of $DHCO^{\bullet+}$ and $DCOH^{\bullet+}$, respectively, with $\sigma_{DHCO^{\bullet+}}$ and $\sigma_{DCOH^{\bullet+}}$ being the reaction CSs for the charge transfer reaction with $CH(CH_3)_3$ for $DHCO^{\bullet+}$ and $DCOH^{\bullet+}$, respectively. Given the endothermicity of the charge transfer process for the $DCOH^{\bullet+}$ isomer with isobutane, $\sigma_{DCOH^{\bullet+}}$ can be assumed to be zero in this case, thereby allowing the fraction of $DHCO^{\bullet+}$ present to be determined as follows:

$$n_{DHCO^{\bullet+}} = \frac{\sigma_T}{\sigma_{DHCO^{\bullet+}}} \quad (4)$$

In order to determine $\sigma_{DHCO^{\bullet+}}$, and under the assumption that there are no kinetic isotope effects so that $\sigma_{DHCO^{\bullet+}}$ is equal to $\sigma_{H_2CO^{\bullet+}}$, we have measured CSs for the reaction of $H_2CO^{\bullet+}$ with isobutane as a function of both photon and collision energy. As mentioned above, this determination of $n_{DCOH^{\bullet+}}$ through subtraction of $n_{DHCO^{\bullet+}}$ is necessitated by the current lack of isomer-selective $DCOH^{\bullet+}$ reactivity data.

For the purpose of a reactivity study with $CH(CH_3)_3$, $H_2CO^{\bullet+}$ ions have been generated via direct ionization of neutral formaldehyde (H_2CO), in turn formed via pyrolysis of paraformaldehyde at 60 °C. The obtained PIE curve around the threshold region for the m/z 30 ($H_2CO^{\bullet+}$) channel is shown in Figure S3 of the Supporting Information, from which an AE for the m/z 30 mass channel of 10.88 ± 0.04 eV has been obtained via linear threshold extrapolation of the PIE curve.[43−46] This is in excellent agreement with the literature IE of H_2CO of 10.889 ± 0.003 eV.[25,26]

https://doi.org/10.1021/acs.jpclett.4c02374
J. Phys. Chem. Lett. 2024, 15, 10888−10895

Absolute reaction CSs as a function of the collision energy have been measured at a photon energy of 11.0 eV in order to limit the impact of internal energy effects while ensuring sufficient reactant ion flux to allow for accurate reactivity measurements. The primary reaction product is that at m/z 58 ($CH(CH_3)_3^{\bullet+}$), corresponding to charge transfer, with absolute CSs for this channel, $\sigma_{H_2CO^{\bullet+}}$, as a function of the collision energy shown in Figure 4. The step function visible in

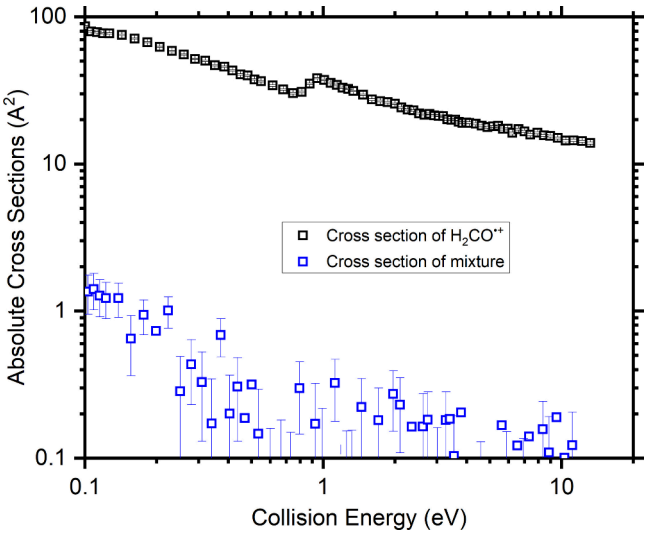

Figure 4. Absolute cross sections (CSs) as a function of the collision energy for the m/z 58 charge transfer product ($CH(CH_3)_3^{\bullet+}$) of the reaction with $CH(CH_3)_3$. Data for the reaction of $H_2CO^{\bullet+}$ generated via direct photoionization of $H_2CO^{\bullet+}$ (black squares) have been recorded at a photon energy of 11.0 eV, while those for the mixture of $DCOH^{\bullet+}$ and $DHCO^{\bullet+}$ ions generated from the dissociative ionization of CD_3OH (blue squares) have been recorded at a photon energy of 13.07 eV.

CS for both channels at a collision energy of ~0.9 eV is due to the "L3 effect", a key indicator of a charge transfer process, with further details given in the Supporting Information. This effect has not been corrected for here as the isomeric fraction is determined from the ratio of the two cross sections, which should remain constant. Although a range of other minor channels are also observed, these are not relevant to the characterization of the isomeric purity and so are not discussed further here.

In order to ensure that $\sigma_{DHCO^{\bullet+}}$ is constant over the 11−12.5 eV photon energy, the CSs for the reaction product at m/z 58 have also been recorded as a function of the photon energy, with the results shown in Figure S4 of the Supporting Information. From this, we note that the measured absolute CSs are approximately independent of the photon energy with only a very slight decrease at higher photon energies, indicating that the absolute CS for this process can be treated as constant with regard to the internal energy of the reactant ions.

Having recorded $\sigma_{H_2CO^{\bullet+}}$, and therefore inferred $\sigma_{DHCO^{\bullet+}}$, σ_T values have been obtained as a function of the collision energy at a photon energy of 13.07 eV, above the 12.52 eV AE of the m/z 31 fragment channel, with the results shown in Figure 4. As with the reaction of $H_2CO^{\bullet+}$, we have also measured the CS for this channel as a function of the photon energy, with results shown in Figure S5 of the Supporting Information. No photon energy dependence for σ_T is observed, allowing the isomeric purity values obtained from the σ_T values recorded at a photon energy of 13.07 eV to be used throughout the 13−15 eV photon energy range.

The values of $n_{DHCO^{\bullet+}}$ obtained from the measured $\sigma_{DHCO^{\bullet+}}$ and σ_T values as a function of the collision energy are shown in Figure 5, while numerical values of $n_{DHCO^{\bullet+}}$, $\sigma_{DHCO^{\bullet+}}$, and σ_T at

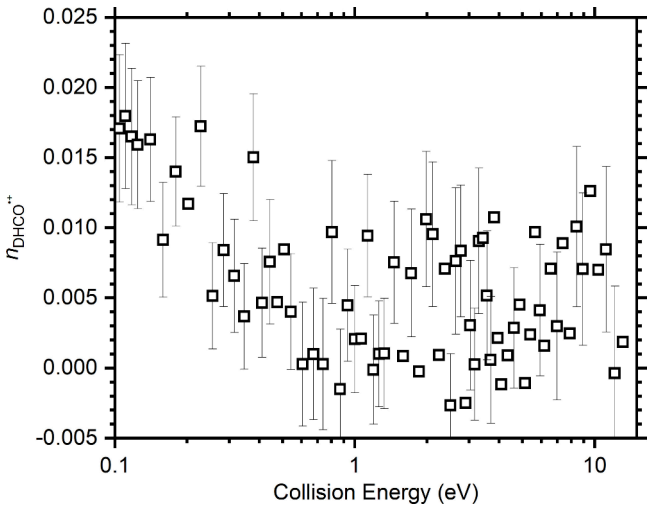

Figure 5. Isomeric fraction of $DHCO^{\bullet+}$, $n_{DHCO^{\bullet+}}$, as a function of the collision energy. This is obtained from σ_T, recorded at a photon energy of 13.07 eV, and $\sigma_{DHCO^{\bullet+}}$, recorded at 11.00 eV, as detailed in the text.

selected collision energies of 0.16, 2.0, and 11.0 eV are given in Table 1. From this, we are able to determine an upper limit for

Table 1. Measured $\sigma_{DHCO^{\bullet+}}$ and σ_T Recorded at Different Collision Energies, along with $n_{DHCO^{\bullet+}}$ Values Determined Using equation 4

Collision Energy (eV)	$\sigma_{DHCO^{\bullet+}}$ (Å²)	σ_T (Å²)	$n_{DHCO^{\bullet+}}$
0.16 ± 0.08	70.90 ± 0.69	0.65 ± 0.28	0.0092 ± 0.0041
2.0 ± 0.08	25.62 ± 0.34	0.27 ± 0.12	0.0105 ± 0.0048
11.0 ± 0.08	14.44 ± 0.25	0.12 ± 0.09	0.0083 ± 0.0064

the $DHCO^{\bullet+}$ fraction at this photon energy of 2.3%, with the average $n_{DHCO^{\bullet+}}$ value over this collision energy range being 0.7 ± 0.5%.

Importantly, the mass spectra of the recorded product ions for the reaction of both $H_2CO^{\bullet+}$ and the m/z 31 fragment of D_3COH (see Figure S2 in the Supporting Information) indicate that the reactivity of the m/z 31 fragment is markedly different from that of the $H_2CO^{\bullet+}$ ion. While detailed consideration of the various reaction processes is beyond the scope of this work, we focus here on the most intense channels from both parent ions. From $H_2CO^{\bullet+}$ these are observed at m/z 58 ($C_4H_{10}^{\bullet+}$ from charge transfer) and at m/z 42 ($C_3H_6^{\bullet+}$ from dissociative charge transfer leading to the loss of CH_4, exothermic by 0.30 eV[26,28]). By contrast, from the m/z 31 fragment from CD_3OH (i.e., $DCOH^{\bullet+}$) the most intense products are at m/z 43 ($C_3H_7^+$ from dissociative proton transfer leading to the loss of CH_4, exothermic by 0.63 eV[26,28]), 57 ($C_4H_9^+$ from dissociative proton transfer leading to the loss of H_2, exothermic by about 0.84 eV[26,28]), and 32 ($DHCOH^+$ formed via hydrogen atom transfer, exothermic by 0.77 eV[26,28]). As the reaction products for this ion are distinct

https://doi.org/10.1021/acs.jpclett.4c02374
J. Phys. Chem. Lett. 2024, 15, 10888−10895

from those of $H_2CO^{\bullet+}$, we conclude that they arise from the reaction of a structurally distinct ionic species which, due to the lack of reasonable alternatives, must be $DCOH^{\bullet+}$.

As no photon energy dependence is observed for the recorded absolute reaction cross sections, we infer that the formation of $DHCO^{\bullet+}$ is energetically accessible from the threshold of the m/z 31 fragment channel and that the isomeric purity is therefore constant over the photon energy range considered here. We tentatively rationalize this observation as the result of efficient H/D scrambling via the interconversion between $CD_3OH^{\bullet+}$ and the isotopic isomers $D_2COHD^{\bullet+}$, $D_2HCOD^{\bullet+}$ and $DHCOD_2^{\bullet+}$, with the fragmentation step being the [1,1] ejection of D_2 from $DHCOD_2^{\bullet+}$. Further in-depth computational investigations are required, complementing the experimental measurements reported here, to allow for a detailed discussion of the different competing pathways. However, we note here that, due to the pathways via H/D exchange, we would expect the isomeric purity to be markedly lower in the case of nondeuterated methanol (CH_3OH) due to the overlap between $H_2CO^{\bullet+}$ and $HCOH^{\bullet+}$ fragmentation channels, thereby significantly removing the need for multiple rearrangements prior to fragmentation to give an isobaric contaminant.

In conclusion, we present experimental characterization of the $HCOH^{\bullet+}$ and $DCOH^{\bullet+}$ ions generated via the dissociative ionization of cyclopropanol and trideuterated methanol, respectively. In contrast to earlier suggestions,[37,38] we find that cyclopropanol is unsuitable for this purpose. However, the generation of $DCOH^{\bullet+}$ from CD_3OH is suitable, with an isomeric purity of 99.3 ± 0.5%. The key finding of this study is that $DCOH^{\bullet+}$ ions generated via the dissociative photoionization of trideuterated methanol (CD_3OH) could be used in future studies to provide important isomer-specific reactivity data for various reaction systems. Such studies are not only essential for the development of accurate models of various astrochemical environments but should also allow for an understanding of the relationship between structure and reactivity that is highly valuable for fundamental reaction dynamics.

■ ASSOCIATED CONTENT

Data Availability Statement

Supporting data can be obtained from DataCat, the University of Liverpool Research Data Catalogue, at 10.17638/datacat.liverpool.ac.uk/2830.

Supporting Information

The Supporting Information is available free of charge at https://pubs.acs.org/doi/10.1021/acs.jpclett.4c02374.

Further details on the experimental methods used in this work as well as the data treatment methods used to correct the data presented in this work; data plots are also provided for which summaries are given in the text (PDF)

■ AUTHOR INFORMATION

Corresponding Author

Vincent Richardson − *Department of Physics, The Oliver Lodge, University of Liverpool, Liverpool L69 7ZE, United Kingdom;* orcid.org/0000-0003-4766-0914; Email: vincent.richardson@liverpool.ac.uk

Authors

Luke Alcock − *Department of Physics, The Oliver Lodge, University of Liverpool, Liverpool L69 7ZE, United Kingdom*

Nicolas Solem − *Université Paris-Saclay, CNRS, Institut de Chimie Physique, UMR8000, 91405 Orsay, France/ Synchrotron SOLEIL, L'Orme de Merisiers, 91190 Saint Aubin, France;* orcid.org/0000-0003-4758-1722

David Sundelin − *Department of Physics, Stockholm University, S-10691 Stockholm, Sweden*

Claire Romanzin − *Université Paris-Saclay, CNRS, Institut de Chimie Physique, UMR8000, 91405 Orsay, France/ Synchrotron SOLEIL, L'Orme de Merisiers, 91190 Saint Aubin, France*

Roland Thissen − *Université Paris-Saclay, CNRS, Institut de Chimie Physique, UMR8000, 91405 Orsay, France/ Synchrotron SOLEIL, L'Orme de Merisiers, 91190 Saint Aubin, France;* orcid.org/0000-0003-0916-2594

Wolf D. Geppert − *Department of Physics, Stockholm University, S-10691 Stockholm, Sweden*

Christian Alcaraz − *Université Paris-Saclay, CNRS, Institut de Chimie Physique, UMR8000, 91405 Orsay, France/ Synchrotron SOLEIL, L'Orme de Merisiers, 91190 Saint Aubin, France*

Miroslav Polášek − *J. Heyrovský Institute of Physical Chemistry of the Czech Academy of Sciences, 182 23 Prague, Czechia*

Brianna R. Heazlewood − *Department of Physics, The Oliver Lodge, University of Liverpool, Liverpool L69 7ZE, United Kingdom;* orcid.org/0000-0003-2073-4004

Quentin Autret − *Université Paris-Saclay, CNRS, Institut de Chimie Physique, UMR8000, 91405 Orsay, France/ Synchrotron SOLEIL, L'Orme de Merisiers, 91190 Saint Aubin, France*

Daniela Ascenzi − *Department of Physics, University of Trento, 38123 Trento, Italy;* orcid.org/0000-0001-5393-9554

Complete contact information is available at: https://pubs.acs.org/10.1021/acs.jpclett.4c02374

Notes

The authors declare no competing financial interest.

■ ACKNOWLEDGMENTS

We thank SOLEIL for providing synchrotron radiation facilities as well as Laurent Nahon and the rest of the facility staff for their assistance in using the DESIRS beamline under Proposal No. 20230262. Furthermore, BRH is grateful to the European Commission (ERC grant no. 948373), and both BRH and VR thank the Leverhulme Trust (grant no. RPG-2022-264) for funding, while LA acknowledges the Department of Physics at the University of Liverpool for final year project funding. WDG and DS acknowledge support from the Swedish research council (grant no. 2019-04332). DA notes that this article is also based upon work from COST Action CA21126 - Carbon molecular nanostructures in space (NanoSpace), supported by COST (European Cooperation in Science and Technology) and acknowledges financial support from MUR PRIN 2020 project no. 2020AFB3FX "Astrochemistry beyond the second period elements" and from the National Recovery and Resilience Plan (NRRP), Mission 4, Component 2, Investment 1.1, Call for tender No. 1409 published on 14.9.2022 by the Italian Ministry of University

and Research (MUR), funded by the European Union − NextGenerationEU − Project Title P20223H8CK "Degradation of space-technology polymers by thermospheric oxygen atoms and ions: an exploration of the reaction mechanisms at an atomistic level" - CUP E53D23015560001. MP acknowledges support from the Czech Ministry of Education, Youth and Sports (grant no. LTC20062). The authors would also like to thank Lucy Morris for her artistry in creating the associated cover art painting.

REFERENCES

(1) Woods, R. C.; Gudeman, C. S.; Dickman, R. L.; Goldsmith, P. F.; Huguenin, G. R.; Irvine, W. M.; Hjalmarson, A.; Nyman, L.-A.; Olofsson, H. The HCO^+/HOC^+ Abundance Ratio in Molecular Clouds. *ApJ* **1983**, *270*, 583−588.
(2) Dohnal, P.; Jusko, P.; Jiménez-Redondo, M.; Caselli, P. Measurements of rate coefficients of CN^+, HCN^+, and HNC^+ collisions with H_2 at cryogenic temperatures. *J. Chem. Phys.* **2023**, *158*, 244303.
(3) Petrie, S.; Freeman, C. G.; McEwan, M. J.; Ferguson, E. E. The ion chemistry of HNC^+/HCN^+ isomers: astrochemical implications. *Mon. Not. R. Astron. Soc.* **1991**, *248*, 272−275.
(4) Hansel, A.; Glantschnig, M.; Scheiring, C.; Lindinger, W.; Ferguson, E. E. Energy dependence of the isomerization of HCN^+ to HNC^+ via ion molecule reactions. *J. Chem. Phys.* **1998**, *109*, 1743−1747.
(5) Shingledecker, C. N.; Molpeceres, G.; Rivilla, V. M.; Majumdar, L.; Kästner, J. Isomers in Interstellar Environments. I. The Case of Z- and E-cyanomethanimine. *ApJ* **2020**, *897*, 158.
(6) Garcia de la Concepción, J.; Jiménez-Serra, I.; Corchado, J. C.; Molpeceres, G.; Martinez-Henares, A.; Rivilla, V. M.; Colzi, L.; Martín-Pintado, J. A sequential acid-base mechanism in the interstellar medium: The emergence of cis-formic acid in dark molecular clouds. *Astronomy & Astrophysics* **2023**, *675*, A109.
(7) Mathews, L. D.; Adams, N. G. Experimental study of the gas phase chemistry of $C_3H_3^+$ with several cyclic molecules. *Int. J. Mass Spectrom.* **2011**, *299*, 139−144.
(8) Ploenes, L.; Straňák, P.; Mishra, A.; Liu, X.; Pérez-Ríos, J.; Willitsch, S. Collisional alignment and molecular rotation control the chemi-ionization of individual conformers of hydroquinone with metastable Neon. *Nat. Chem.* **2024**, DOI: 10.1038/s41557-024-01590-1. Online ahead of print.
(9) Abma, G. L.; Parkes, M. A.; Horke, D. A. Preparation of Tautomer-Pure Molecular Beams by Electrostatic Deflection. *J. Phys. Chem. Lett.* **2024**, *15*, 4587−4592.
(10) Xu, L.; Toscano, J.; Willitsch, S. Trapping and Sympathetic Cooling of Conformationally Selected Molecular Ions. *Phys. Rev. Lett.* **2024**, *132*, 083001.
(11) Mishra, A.; Kim, J.; Kim, S. K.; Willitsch, S. Isomeric and rotational effects in the chemi-ionisation of 1,2-dibromoethene with metastable neon atoms. *Faraday Discuss.* **2024**, *251*, 92−103.
(12) Parker, K.; Bollis, N. E.; Ryzhov, V. Ion−molecule reactions of mass-selected ions. *Mass Spectrom. Rev.* **2024**, *43*, 47−89.
(13) Liu, J. K.-Y.; Niyonsaba, E.; Alzarieni, K. Z.; Boulos, V. M.; Yerabolu, R.; Kenttämaa, H. I. Determination of the compound class and functional groups in protonated analytes via diagnostic gas-phase ion−molecule reactions. *Mass Spectrom. Rev.* **2023**, *42*, 1508−1534.
(14) Richardson, V.; Alcaraz, C.; Geppert, W. D.; Polášek, M.; Romanzin, C.; Sundelin, D.; Thissen, R.; Tosi, P.; Žabka, J.; Ascenzi, D. The reactivity of methanimine radical cation ($H_2CNH^{\bullet+}$) and its isomer aminomethylene ($HCNH_2^{\bullet+}$) with methane. *Chem. Phys. Lett.* **2021**, *775*, 138611.
(15) Liu, J.; Van Devener, B.; Anderson, S. L. Reaction of formaldehyde cation with methane: Effects of collision energy and H_2CO^+ and methane vibrations. *J. Chem. Phys.* **2003**, *119*, 200−214.
(16) Liu, J.; Van Devener, B.; Anderson, S. L. Vibrational mode and collision energy effects on reaction of H_2CO^+ with C_2D_4. *J. Chem. Phys.* **2004**, *121*, 11746−11759.
(17) Chamot-Rooke, J.; Mourgues, P.; van der Rest, G.; Audier, H. E. Ambient reactivity and characterization of small ionized carbenes. *Int. J. Mass Spectrom.* **2003**, *226*, 249−269.
(18) Sundelin, D.; Ascenzi, D.; Richardson, V.; Alcaraz, C.; Polášek, M.; Romanzin, C.; Thissen, R.; Tosi, P.; Žabka, J.; Geppert, W. D. The reactivity of methanimine radical cation ($H_2CNH^{\bullet+}$) and its isomer aminomethylene ($HCNH_2^{\bullet+}$) with C_2H_4. *Chem. Phys. Lett.* **2021**, *777*, 138677.
(19) Richardson, V.; Ascenzi, D.; Sundelin, D.; Alcaraz, C.; Romanzin, C.; Thissen, R.; Guillemin, J.-C.; Polášek, M.; Tosi, P.; Žabka, J.; Geppert, W. D. Experimental and Computational Studies on the Reactivity of Methanimine Radical Cation ($H_2CNH^{\bullet+}$) and its Isomer Aminomethylene ($HCNH_2^{\bullet+}$) With C_2H_2. *Front. Astron. Space Sci.* **2021**, *8*, 752376.
(20) Snyder, L. E.; Buhl, D.; Zuckerman, B.; Palmer, P. Microwave Detection of Interstellar Formaldehyde. *Phys. Rev. Lett.* **1969**, *22*, 679−681.
(21) Gerin, M.; Liszt, H.; Pety, J.; Faure, A. H_2CO and CS in diffuse clouds: Excitation and abundance. *Astronomy & Astrophysics* **2024**, *686*, A49.
(22) Pegues, J.; et al. An ALMA Survey of H_2CO in Protoplanetary Disks. *ApJ.* **2020**, *890*, 142.
(23) Tenenbaum, E. D.; Milam, S. N.; Woolf, N. J.; Ziurys, L. M. Molecular Survival In Evolved Planetary Nebulae: Detection of H_2CO, c-C_3H_2, and C_2H In the Helix. *ApJ* **2009**, *704*, L108−L112.
(24) Ramal-Olmedo, J. C.; Menor-Salván, C. A.; Fortenberry, R. C. Mechanisms for gas-phase molecular formation of neutral formaldehyde (H_2CO) in cold astrophysical regions. *Astronomy & Astrophysics* **2021**, *656*, A148.
(25) Niu, B.; Shirley, D. A.; Bai, Y. High resolution photoelectron spectroscopy and femtosecond intramolecular dynamics of H_2CO^+ and D_2CO^+. *J. Chem. Phys.* **1993**, *98*, 4377−4390.
(26) Linstrom, P. J.; Mallard, W. G. NIST Chemistry WebBook - Standard Reference Database n. *69*. [Online], accessed May 2024; http://webbook.nist.gov.
(27) Zanchet, A.; García, G. A.; Nahon, L.; Bañares, L.; Marggi Poullain, S. Signature of a conical intersection in the dissociative photoionization of formaldehyde. *Phys. Chem. Chem. Phys.* **2020**, *22*, 12886−12893.
(28) Ruscic, B.; Bross, D. Active Thermochemical Tables (ATcT) values based on ver. 1.124 of the Thermochemical Network. [Online], 2024.
(29) Wagner, J. P.; Barlett, M. A.; Allen, W. D.; Duncan, M. A. Tunneling Isomerizations on the Potential Energy Surfaces of Formaldehyde and Methanol Radical Cations. *ACS Earth Space Chem.* **2017**, *1*, 361−367.
(30) Snyder, L. E.; Hollis, J. M.; Ulich, B. L. Radio detection of the interstellar formyl radical. *ApJ* **1976**, *208*, L91−L94.
(31) Ohishi, M.; Ishikawa, S. I.; Amano, T.; Oka, H.; Irvine, W. M.; Dickens, J. E.; Ziurys, L. M.; Apponi, A. J. Detection of A New Interstellar Molecular Ion, H_2COH^+ (Protonated Formaldehyde). *ApJ* **1996**, *471*, L61.
(32) Ball, J. A.; Gottlieb, C. A.; Lilley, A. E.; Radford, H. E. Detection of Methyl Alcohol in Sagittarius. *ApJ* **1970**, *162*, L203.
(33) Richardson, V.; Valença Ferreira de Aragão, E.; He, X.; Pirani, F.; Mancini, L.; Faginas-Lago, N.; Rosi, M.; Martini, L. M.; Ascenzi, D. Fragmentation of interstellar methanol by collisions with $He^{\bullet+}$: an experimental and computational study. *Phys. Chem. Chem. Phys.* **2022**, *24*, 22437−22452.
(34) Schulenburg, A. M.; Meisinger, M.; Radi, P. P.; Merkt, F. The formaldehyde cation: Rovibrational energy level structure and Coriolis interaction near the adiabatic ionization threshold. *J. Mol. Spectrosc.* **2008**, *250*, 44−50.
(35) Liu, J.; Kim, H.-T.; Anderson, S. L. Multiphoton ionization and photoelectron spectroscopy of formaldehyde via its 3*p* Rydberg states. *J. Chem. Phys.* **2001**, *114*, 9797−9806.
(36) Hockey, E. K.; McLane, N.; Martí, C.; Duckett, L.; Osborn, D. L.; Dodson, L. G. Direct Observation of Gas-Phase Hydroxy-

methylene: Photoionization and Kinetics Resulting from Methanol Photodissociation. *J. Am. Chem. Soc.* **2024**, *146*, 14416−14421.
(37) Wesdemiotis, C.; McLafferty, F. W. Mass Spectral Evidence for the Hydroxymethylene Radical Cation. *Tetrahedron Lett.* **1981**, *22*, 3479−3480.
(38) Burgers, P. C.; Mommers, A. A.; Holmes, J. L. Ionized Oxycarbenes: $[COH]^+$, $[HCOH]^{+\bullet}$, $[C(OH)_2]^{+\bullet}$, $[HCO_2]^+$, and $[COOH]^+$, Their Generation, Identification, Heat of Formation, and Dissociation Characteristics. *J. Am. Chem. Soc.* **1983**, *105*, 5976−5979.
(39) Mauney, D. T.; Mosley, J. D.; Madison, L. R.; McCoy, A. B.; Duncan, M. A. Infrared spectroscopy and theory of the formaldehyde cation and its hydroxymethylene isomer. *J. Chem. Phys.* **2016**, *145*, 174303.
(40) Berkowitz, J. Photoionization of CH_3OH, CD_3OH and CH_3OD: Dissociative ionization mechanisms and ionic structures. *J. Chem. Phys.* **1978**, *69*, 3044−3054.
(41) Nahon, L.; de Oliveira, N.; Garcia, G. A.; Gil, J.-F.; Pilette, B.; Marcouillé, O.; Lagarde, B.; Polack, F. DESIRS: a state-of-the-art VUV beamline featuring high resolution and variable polarization for spectroscopy and dichroism at SOLEIL. *J. Synchrotron Radiat.* **2012**, *19*, 508−520.
(42) Bombach, R.; Dannacher, J.; Honegger, E.; Stadelmann, J.-P.; Neier, R. Unimolecular Dissociations of Excited $C_3H_6O^+$: A Photoelection-Photoion Coincidence Study of Cyclopropanol and Allyl Alcohol. *Chem. Phys.* **1983**, *82*, 459−470.
(43) Roithová, J.; Schröder, D.; Loos, J.; Schwarz, H.; Jankowiak, H.-C.; Berger, R.; Thissen, R.; Dutuit, O. Revision of the second ionization energy of toluene. *J. Chem. Phys.* **2005**, *122*, 094306.
(44) Chupka, W. A. Effect of Thermal Energy on Ionization Efficiency Curves of Fragment Ions. *J. Chem. Phys.* **1971**, *54*, 1936−1947.
(45) Traeger, J. C.; McLoughlin, R. G. Absolute heats of formation for gas-phase cations. *J. Am. Chem. Soc.* **1981**, *103*, 3647−3652.
(46) Castrovilli, M. C.; Bolognesi, P.; Cartoni, A.; Catone, D.; O'Keefe, P.; Casavola, A. R.; Turchini, S.; Zema, N.; Avaldi, L. Photofragmentation of Halogenated Pyrimidine Molecules in the VUV Range. *J. Am. Soc. Mass Spectrom.* **2014**, *25*, 351−367.
(47) Ruscic, B. Photoionization Mass Spectroscopic Studies of Free Radicals in Gas Phase: Why and How. *Res. Adv. Phys. Chem.* **2000**, *1*, 39−75.
(48) Kim, J. K.; Anicich, V. G.; Huntress, Jr. W. T. Product distributions and rate constants for the reactions of CH_3^+, CH_4^+, $C_2H_2^+$, $C_2H_3^+$, $C_2H_4^+$, $C_2H_5^+$, and $C_2H_6^+$ ions with CH_4, C_2H_2, C_2H_4, and C_2H_6. *J. Phys. Chem.* **1977**, *81*, 1798−1805.
(49) Ervin, K. M.; Armentrout, P. B. Translational energy dependence of $Ar^+ + XY \rightarrow ArX^+ + Y$ (XY = H_2, D_2, HD) from thermal to 30 eV c.m. *J. Chem. Phys.* **1985**, *83*, 166−189.
(50) Nicolas, C.; Alcaraz, C.; Thissen, R.; Žabka, J.; Dutuit, O. Effects of ion excitation on charge transfer reactions of the Mars, Venus, and Earth ionospheres. *Plan. Space Sci.* **2002**, *50*, 877−887.
(51) Borkar, S.; Sztáray, B.; Bodi, A. Dissociative photoionization mechanism of methanol isotopologues (CH_3OH, CD_3OH, CH_3OD and CD_3OD) by iPEPICO: energetics, statistical and non-statistical kinetics and isotope effects. *Phys. Chem. Chem. Phys.* **2011**, *13*, 13009−13020.

https://doi.org/10.1021/acs.jpclett.4c02374
J. Phys. Chem. Lett. 2024, 15, 10888−10895